

## Direct Investigation of Superparamagnetism in Co Nanoparticle Films

S. I. Woods, J. R. Kirtley, Shouheng Sun, and R. H. Koch

*IBM T. J. Watson Research Center, Yorktown Heights, New York 10598*

(Received 7 May 2001; published 10 September 2001)

A direct probe of superparamagnetism was used to determine the complete anisotropy energy distribution of Co nanoparticle films. The films were composed of self-assembled lattices of uniform Co nanoparticles of 3 or 5 nm in diameter, and a variable temperature scanning-SQUID microscope was used to measure temperature-induced spontaneous magnetic noise in the samples. Accurate measurements of anisotropy energy distributions of small volume samples will be critical to magnetic optimization of nanoparticle devices and media.

DOI: 10.1103/PhysRevLett.87.137205

PACS numbers: 75.50.Tt, 05.40.Ca, 65.80.+n, 75.20.-g

There has been a recent explosion of research into the fabrication and understanding of assemblies of magnetic nanoparticles [1–7]. Increasing ability to controllably produce superlattices of these nanoparticles with uniform material properties will have important consequences on technology and our basic comprehension of magnetism. Technologically, nanoparticle films with sharp distributions of magnetic properties can be used to tailor nanodevices and high-density recording media with reliable, reproducible characteristics. Scientifically, a uniform array of identical particles is an ideal model system for the study of single particle and interparticle magnetic properties, without interference from broad or irregular volume and lattice-spacing distributions.

Although most magnetic nanoparticle technological applications depend on the ferromagnetic state of the particles, understanding their superparamagnetic state is crucial to controlling their behavior. For nanoparticles, very small absolute deviations in particle size can lead to large changes in blocking temperature, interfering with device function at operational temperatures. Fundamental magnetic parameters such as anisotropy energy and flipping times can be extracted from superparamagnetic data [8–11], and these parameters can in turn be used to predict the magnetic response of a sample or device. Superparamagnetic behavior is a primary enemy to faithful operation of nanodevices and nanoparticle memories, so it is vital that an accurate and complete method for extracting magnetic distributions from nanoparticle systems be developed. With such methods, magnetic optimization of these technologies will be hastened.

We have directly probed superparamagnetism in films of self-assembled cobalt nanoparticles by measuring the spontaneous magnetic noise arising from these films as a function of temperature, a method some have pursued to measure nanoparticle properties [12]. Nanoparticle spin flips, induced by thermal energy, are directly sensed by a micro-SQUID, giving statistical information on the magnetic properties of millions of particles in the array. Not only can the average anisotropy energy and width be determined, but it is shown below how the entire magnetic anisotropy energy distribution can be extracted, a complete

magnetic fingerprint. The extracted distribution is shown to be self-consistent, closely reproducing the data from which it was derived. The micro-SQUID noise technique described here is ideally suited for the statistical study of nanoparticle films because it can determine the anisotropy distribution without requiring the easy axes of the nanoparticles to be aligned and has the magnetization sensitivity to investigate submicron area samples only a nanometer thick.

The samples investigated were films of Co nanoparticles deposited on thermally oxidized silicon substrates. Monodisperse Co nanoparticles with the multiply twinned face-centered cubic structure (mt-fcc structure [13]) were prepared using high-temperature solution-phase synthesis [14]. The size of the nanoparticles can be controlled by the details of synthesis and separation techniques, and TEM studies indicate  $\sigma < 5\%$  for the diameter distributions of these particles. Each nanoparticle was produced with an oleic acid coat of 2 nm thickness which served to stabilize the particles, prevent oxidation, and control interparticle spacing. The nanoparticles were dispersed in hexane and deposited on oxidized silicon substrates, where the hexane was allowed to slowly evaporate, leaving 5–10 layers of particles. The Co nanoparticles self-assemble on the substrates into close-packed arrays with lattice spacing approximately  $(d + 4 \text{ nm})$ , where  $d$  is the diameter of the nanoparticles. In this study, samples with nominal nanoparticle diameters of 3 and 5 nm were investigated. Figure 1 shows a TEM image of a superlattice of 5 nm particles on a thin layer of silicon oxide.

Samples were measured using a variable temperature scanning-SQUID microscope, employing a niobium SQUID with an integrated  $17.8 \mu\text{m}$  square pickup loop [15]. This SQUID was modulated at 100 kHz using a standard flux modulation and feedback method. The ac output from the SQUID electronics was fed into an HP35665A digital signal analyzer to study the magnetic activity of the nanoparticles at frequencies from 10–10 000 Hz and temperatures from 4–100 K. The power spectral density of the SQUID output voltage was recorded and could be easily converted to find the magnetic noise power density produced by the sample. The SQUID could be moved

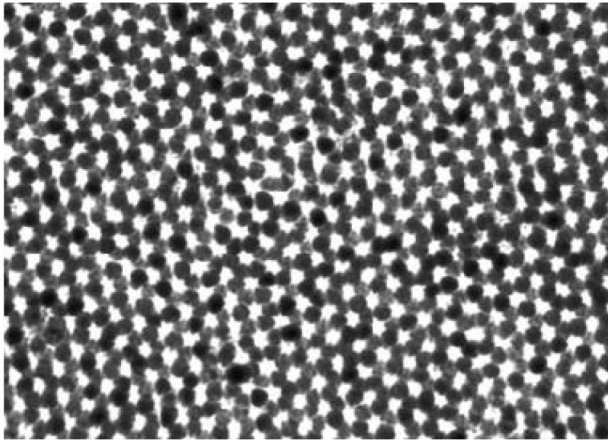


FIG. 1. TEM micrograph of a self-assembled superlattice of 5 nm diameter Co nanoparticles on silicon oxide. An oleic acid coat of 2 nm around each particle leads to a superlattice spacing of approximately 9 nm between particle centers.

into and out of contact with the sample, so background signals and the frequency response of the SQUID could be separated from the sample signal. Measurements were made in a shielded room and the sample space had ambient fields of about 1  $\mu$ T. Data were taken in near contact with the nanoparticles ( $\sim 3$   $\mu$ m away) and at heights of 100–500  $\mu$ m. In addition, the magnetization-temperature curves of the samples were characterized with a Quantum Magnetics MPMS system before execution of the noise measurement.

In the simple case of a bistable, single-domain particle with no interactions, the magnetic noise power measured at temperature  $T$ , cyclic frequency  $\omega$ , and distance  $d$  away is [16,17]

$$S_B(\omega, T) = \left( \frac{\mu_o}{4\pi} \frac{MV}{d^3} \right)^2 \frac{\tau}{1 + \omega^2 \tau^2}, \quad (1)$$

where  $M$  is the particle magnetization,  $V$  is the particle volume, and  $\tau$  is the average cyclic flipping time for the moment. This flipping time follows the standard activated form  $\tau = \tau_o \exp(U/k_B T)$ , where  $U$  is the anisotropy energy of the particle;  $U = KV$ , where  $K$  is the effective anisotropy constant. The noise power is flat at low frequencies with a falloff near  $\tau^{-1}$ . As a function of temperature,  $S_B$  displays a single peak centered at  $T_{\text{peak}} = -U/k_B \log(\omega \tau_o)$ . Simply put,  $S_B(T)$  peaks when the measurement frequency equals the inverse flipping time, i.e., when  $\omega = \tau^{-1} = \tau_o^{-1} \exp(-U/k_B T)$ .

For a distribution  $D(U)$  of particle anisotropy energies, one finds for the noise power [approximating with use of an average prefactor to the Lorentzian in Eq. (1)]:

$$S_B(\omega, T) \propto \int_0^\infty \frac{\tau_o e^{U/k_B T}}{1 + \omega^2 \tau_o^2 e^{2U/k_B T}} D(U) dU. \quad (2)$$

A peaked distribution will exhibit a peaked noise power as a function of temperature, just as in the single particle

case, but the peak will be broadened. Approximate average values  $\bar{\tau}_o$  and  $\bar{U}$  for the flipping time and anisotropy energy can be found by assuming this peak occurs at  $T_{\text{peak}} = -\bar{U}/k_B \log(\omega \bar{\tau}_o)$ .

Results of noise power as a function of frequency from a film of 5 nm diameter nanoparticles are shown for various temperatures in Fig. 2. As expected, noise decreases monotonically in the frequency window for each particular temperature, having an approximate form of  $S_B \propto f^{-\alpha}$ . For the 5 nm nanoparticles,  $\alpha$  decreases from about 1.0 to 0.6 as temperature is increased from 25 to 85 K, as shown in the inset of Fig. 2. Noise power as a function of temperature for both 3 and 5 nm diameter nanoparticle samples is shown in Fig. 3 for various frequencies. Each curve peaks at a temperature that increases as the measurement frequency increases. The 3 nm sample peaks near  $T = 20$  K, and the 5 nm sample peaks near  $T = 55$  K. These temperatures approximate the average superparamagnetic blocking temperature for each sample and agree with the peak location in the zero-field-cooled magnetization-temperature curves measured on each sample. In the following analysis, it is assumed that the noninteracting form of the equations for  $S_B$  and  $\tau$  (with  $\tau_o$  and  $U$  possibly renormalized by interactions) is sufficient to describe the behavior of the system.

Average values for  $\tau_o$  and  $U$  can be extracted from the noise data peak locations as discussed above, and a least squares fit was made of the  $\log(\omega)$  vs  $T_{\text{peak}}^{-1}$  data to find these parameters for the two samples. For the 3 nm particles, the attempt time  $2\pi\tau_o$  and anisotropy energy  $\bar{U}$  are  $2.16 \times 10^{-11}$  s and  $5.22 \times 10^{-21}$  J, respectively. The average attempt time is  $5.22 \times 10^{-11}$  s and average

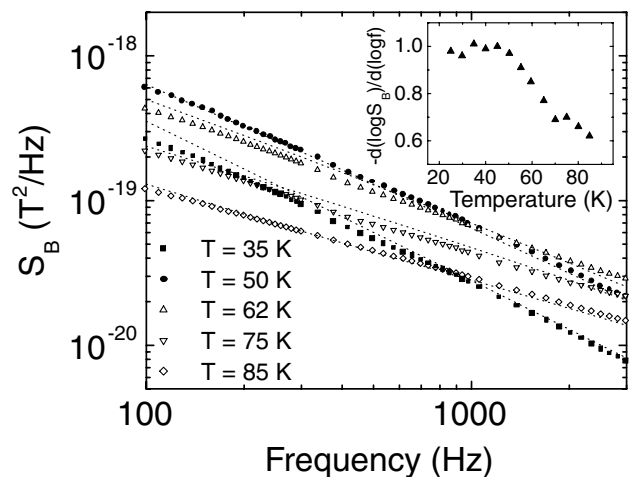


FIG. 2. Magnetic noise power as a function of frequency at numerous temperatures for a film of 5 nm diameter nanoparticles. The fitting curves were generated from an extracted distribution of anisotropy energies. The general form of the data is approximately  $S_B \propto f^{-\alpha}$ , and the inset shows the value of  $\alpha$  as a function of temperature for this sample.

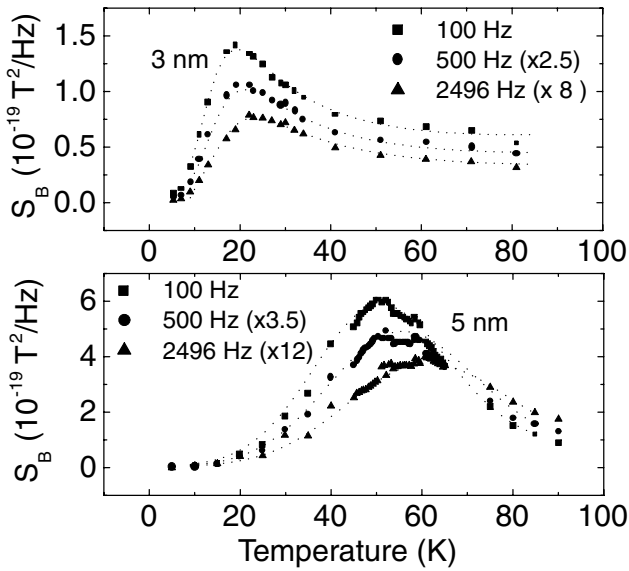


FIG. 3. Magnetic noise power as a function of temperature at three frequencies for films of 3 nm (top panel) and 5 nm (bottom panel) diameter nanoparticles. The fitting curves were generated from extracted distributions of anisotropy energies.

anisotropy energy is  $1.35 \times 10^{-20}$  J for the 5 nm particles. In the determination of the full energy distribution to follow, the only input parameter will be the approximate value calculated for the attempt time [18].

By rewriting Eq. (2) as an infinite series, the complete anisotropy energy can be easily extracted from the noise power data under certain conditions. Let  $F(U) = \frac{\tau_o e^{U/k_B T}}{1 + \omega^2 \tau_o^2 e^{2U/k_B T}}$ , then Eq. (2) can be expressed as  $S_B(\omega, T) \propto \int_0^\infty F(U) D(U) dU$ .  $F(U)$  is a function peaked at  $\tilde{U} = -k_B T \log(\omega \tau_o)$  with width of approximately  $k_B T$ , falling quickly to zero outside this window.  $D(U)$  is slowly varying with respect to  $k_B T$  in this region. Expanding  $D(U)$  in a power series and evaluating the  $F(U)$ -containing integrals (integrals of the form  $\int_0^\infty \frac{x^{2n}}{\cosh(ax)} dx$  [19]), one finds [20]

$$S_B(\omega, T) \propto \frac{1}{\omega} \sum_{n=0}^{\infty} \frac{|E_{2n}|}{(2n)!} \left( \frac{\pi k_B T}{2} \right)^{2n+1} D^{(2n)}(\tilde{U}), \quad (3)$$

where  $E_m$  is the  $m$ th Euler number. As long as  $D(U)$  is very slowly varying over a scale of  $k_B T$  around  $\tilde{U}$  [the width of  $D(U)$  is much more than  $k_B T$  around  $\tilde{U}$ ], the first term alone will give a good approximation of the noise power. Thus, the distribution can be found from the noise power according to

$$D(-k_B T \log(\omega \tau_o)) \propto \frac{2\omega}{\pi k_B T} S_B(\omega, T). \quad (4)$$

If this approximation was not good enough, an iterative procedure using higher order terms could be used to calculate  $D(U)$  from the noise power.

The noise power data as a function of temperature for both the 3 and the 5 nm samples were used to derive their

anisotropy energy distributions, according to Eq. (4). At each frequency the distribution was calculated and normalized to make the total probability under the distribution equal to unity. Figure 4 shows all the data for numerous frequencies plotted together. For each sample, the data define a single universal curve, the anisotropy energy distribution. The distribution for the 3 nm particles reaches a peak at  $4.35 \times 10^{-21}$  J, has a full width half maximum (FWHM) of about 110%, and has a tail at high energies. For the 5 nm particles, the distribution is more symmetric, has a peak at  $1.22 \times 10^{-20}$  J, and a FWHM of about 64%.

To demonstrate the reliability of these extracted distributions, it is important to show they can reproduce the data from which they were derived. By plugging the derived distributions into Eq. (2), one can generate the calculated form for the noise power. The dotted lines in Figs. 2 and 3 show these generated curves, and they provide excellent fits to all the data.

The derived energy distributions are wider than the apparent volume distributions, which generally appear Gaussian with  $\sigma < 15\%$  (FWHM  $< 35\%$ ). As it is more difficult to stabilize uniform smaller particles, it is not surprising that the distribution for the 3 nm particles is wider than that of the 5 nm particles and shows a tail indicative of a noticeable fraction of larger diameter particles. If one assumes the energy peak for each sample is that of a single-domain, spherical nanoparticle of the nominal diameter, then  $K_{3\text{nm}} = 3.08 \times 10^5$  J/m<sup>3</sup> and  $K_{5\text{nm}} = 1.87 \times 10^5$  J/m<sup>3</sup>, in general agreement with other values derived for mt-fcc Co nanoparticles [21,22]. It is believed that surface anisotropy dominates in near-spherical nanoparticles (and is uniaxial, even for cubic crystal structures), and in this case the anisotropy constant is expected to scale as the inverse of particle

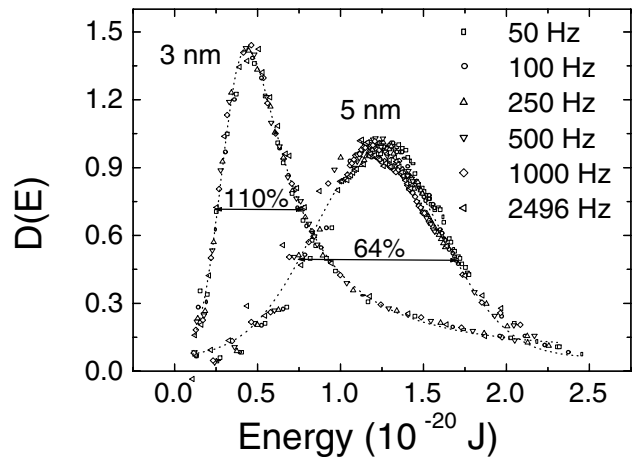


FIG. 4. Extracted anisotropy energy distributions for films of 3 and 5 nm diameter nanoparticles. The 3 nm curve is peaked at  $4.35 \times 10^{-21}$  J and exhibits a high energy tail. The 5 nm distribution is peaked at  $1.22 \times 10^{-20}$  J and is symmetric, being well fit by a Gaussian curve (dotted line).

diameter [23,24]. In this study the nominal ratio of the inverse particle diameters of the two types of samples measured is 1.67, while the ratio in anisotropy constants is 1.65, in good agreement with the relation expected for surface anisotropy. Various reasons could account for energy distributions significantly wider than nanoparticle volume distributions, including existence of nonuniformity in the surface anisotropy; the actively magnetic regions of the particles do not correspond with their full TEM-defined sizes; distributions exist in the values of the crystalline, strain, or shape anisotropies across the nanoparticles; or dipolar interactions between nanoparticles are significant.

We investigated the possible effects of dipolar interactions on the nanoparticle films through Monte Carlo simulations on close-packed monolayers of particles. The nanoparticles are given random easy axis directions and allowed to relax to a low energy state through the rotation and flipping of nanoparticle magnetizations. Results indicate that interparticle dipolar energies are relatively insignificant in the case of the 3 nm particles but could account for about 15% of the full width spread in the flipping energy distribution of the 5 nm particles. In the case where the 5 nm particles are given a Gaussian diameter distribution with  $\sigma = 5\%$ , the simulation renders an anisotropy energy distribution with a width of 51%, accounting for a significant part of the 64% width measured on the 5 nm diameter sample.

We have presented data gathered by a direct probe of superparamagnetism in a magnetic nanoparticle system. The noise power technique with a variable temperature micro-SQUID can be used to extract precise magnetic energy information on technologically important magnetic nanoparticle films and devices of small area and thickness. Even for films with sharp volume distributions of nanoparticles, our magnetic measurement shows that the magnetic distributions can be relatively wide. Thus, such a technique is essential to optimize particle growth conditions for magnetic uniformity, critical for any application. A similar scanning-SQUID microscope system employing a high- $T_c$  SQUID could be used to characterize films at room temperature. The noise measurement technique also holds promise as a sensitive method to probe and understand interactions in nanoparticle superlattices as the interparticle spacing is changed.

[1] S. Sun, C. B. Murray, D. Weller, L. Folks, and A. Moser, *Science* **287**, 1989 (2000).

[2] E. E. Carpenter, J. A. Sims, J. A. Wienmann, W. L. Zhou, and C. J. O'Connor, *J. Appl. Phys.* **87**, 5615 (2000).

[3] C. Stamm *et al.*, *Science* **282**, 449 (1998).

[4] H. Mamiya, I. Nakatani, and T. Furubayashi, *Phys. Rev. Lett.* **84**, 6106 (2000).

[5] C. T. Black, C. B. Murray, R. L. Sandstrom, and S. Sun, *Science* **290**, 1131 (2000).

[6] W. Wernsdorfer *et al.*, *Phys. Rev. Lett.* **78**, 1791 (1997).

[7] J. L. Dormann, D. Fiorani, and E. Tronc, *Adv. Chem. Phys.* **98**, 283 (1997).

[8] C. P. Bean and J. D. Livingston, *J. Appl. Phys.* **30**, 120S (1959).

[9] C. Petit and M. P. Pileni, *Appl. Surf. Sci.* **162–163**, 519 (2000).

[10] J. van Lierop and D. H. Ryan, *Phys. Rev. Lett.* **85**, 3021 (2000).

[11] T. Jonsson, J. Mattsson, P. Nordblad, and P. Svedlindh, *J. Magn. Mater.* **168**, 269 (1997).

[12] T. Jonsson, P. Nordblad, and P. Svedlindh, *Phys. Rev. B* **57**, 497 (1998).

[13] S. Ino, *J. Phys. Soc. Jpn.* **21**, 346 (1966).

[14] S. Sun and C. B. Murray, *J. Appl. Phys.* **85**, 4325 (1999). The 3 nm cobalt nanoparticle dispersion was synthesized by mixing dicobalt octacarbonyl (342 mg, 1 mmol), phenyl ether (20 mL), tributylphosphine (0.3 mL, 1 mmol), and oleic acid (0.32 mL, 1 mmol) under airless conditions at 200 °C. The procedure for synthesis was similar to that described in Ref. [1]. The 5 nm cobalt particles were synthesized in much the same way by adjusting the molar ratios of dicobalt octacarbonyl, tributylphosphine, and oleic acid to 1/0.5/0.5.

[15] J. R. Kirtley *et al.*, *Appl. Phys. Lett.* **74**, 4011 (1999).

[16] Sh. Kogan *et al.*, *Electronic Noise and Fluctuations in Solids* (Cambridge University Press, New York, 1996), p. 33.

[17] M. J. Buckingham, *Noise in Electronic Devices and Systems* (Ellis Horwood Limited, New York, 1983), p. 33.

[18] In the linear fits, the standard errors for  $\log(\tau_o)$  are  $\sim 11\%$  for the 3 nm particles and  $\sim 6\%$  for the 5 nm particles, implying the error for  $\tau_o$  can be about an order of magnitude. This possible error has only a small effect on the calculated distribution results, however. In the extraction, the input value of  $\tau_o$  affects only the energy scaling (multiplies the energy scale by a constant value at each frequency) and not the shape of the distribution. A change of  $\tau_o$  by a factor of 10 leads to a change in energy of  $\sim 13\%$ .

[19] I. S. Gradshteyn and I. M. Ryzhik, *Table of Integrals, Series, and Products* (Academic Press, New York, 1980), p. 349.

[20] P. Dutta, P. Dimon, and P. M. Horn, *Phys. Rev. Lett.* **43**, 646 (1979).

[21] J. P. Chen, C. M. Sorensen, K. J. Klabunde, and G. C. Hadjipanayis, *Phys. Rev. B* **51**, 11 527 (1995).

[22] M. Jamet *et al.*, *Phys. Rev. Lett.* **86**, 4676 (2001).

[23] F. Bodker, S. Morup, and S. Linderoth, *Phys. Rev. Lett.* **72**, 282 (1994).

[24] F. Bodker and S. Morup, *Europhys. Lett.* **52**, 217 (2000).